

## Regular article

# Enhanced thermoelectric properties of bismuth telluride bulk achieved by telluride-spilling during the spark plasma sintering process



Zhen-Hua Ge<sup>a,\*</sup>, Yi-Hong Ji<sup>a</sup>, Yang Qiu<sup>b</sup>, Xiaoyu Chong<sup>a</sup>, Jing Feng<sup>a</sup>, Jiaqing He<sup>b,\*</sup>

<sup>a</sup> Faculty of Materials Science and Engineering, Kunming University of Science and Technology, Kunming 650093, China

<sup>b</sup> Shenzhen Key Laboratory of Thermoelectric Materials, Department of Physics, South University of Science and Technology of China, Shenzhen 518055, China

## ARTICLE INFO

## Article history:

Received 21 August 2017

Received in revised form 12 September 2017

Accepted 12 September 2017

Available online xxxx

## Keywords:

Thermoelectric

Bi<sub>2</sub>Te<sub>3</sub>

Mechanical alloying

Spark plasma sintering

Dislocations

## ABSTRACT

We offered a new and simple routine for significant reducing lattice thermal conductivity and improve the thermoelectric properties of Bi<sub>2</sub>Te<sub>3</sub> materials. Dense dislocations were introduced by means of adding excess Te into Bi<sub>2</sub>Te<sub>3</sub> powder by combining ball milling and spark plasma sintering (SPS). During the high temperature SPS process, excess Te spilled out of the die. The ultra-low lattice thermal conductivity of Bi<sub>2</sub>Te<sub>3</sub> was achieved due to the enhanced phonon scattering by dislocations. The highest ZT value of 0.7 at 398 K was obtained for a pure Bi<sub>2</sub>Te<sub>3</sub> bulk sample which is 175% higher than that of pristine Bi<sub>2</sub>Te<sub>3</sub> sample.

© 2017 Acta Materialia Inc. Published by Elsevier Ltd. All rights reserved.

The global demand for affordable and renewable energy resources has led to important approaches including thermoelectric (TE) energy conversion. The efficiency of thermoelectric materials determined by the dimensionless figure of merit  $ZT = \alpha^2 \sigma T / \kappa$ , where  $\alpha$  is the Seebeck coefficient,  $\sigma$  is the electrical conductivity,  $T$  is the absolute temperature and  $\kappa$  is the thermal conductivity which consists of electrical thermal conductivity  $\kappa_e$  and lattice thermal conductivity  $\kappa_L$ . The main challenge for enhance thermoelectric properties lies in simultaneously increase both Seebeck coefficient  $\alpha$ , electrical conductivity  $\sigma$  and reduce the thermal conductivity  $\kappa$  [1–5].

Heat-carrying carriers cover a broad spectrum of frequencies ( $\omega$ ) and the lattice thermal conductivity can be expressed as a sum of contribution from different frequencies:  $\kappa_L = \int \kappa_s(\omega) d\omega$  [6]. Different scattering mechanisms target on different frequencies phonons, be it Umklapp scattering that generally has a  $\tau_u^{-1} \sim \omega^2$ , point-defect scattering and boundary scattering target high frequency phonons ( $(\tau_{PD}^{-1} \sim \omega^4)$ ) and low frequency phonons (as it is frequency independent  $\tau_B^{-1} \sim \text{constant}$ ) respectively [7].

Bismuth telluride (Bi<sub>2</sub>Te<sub>3</sub>) based compounds belong to class of a layered semiconductors and are the best TE materials available today near room temperature with the highest dimensionless figure of merit ZT of beyond 1 [8–10]. However, the pure Bi<sub>2</sub>Te<sub>3</sub> (n-type) without chemical doping, especially prepared by the solution phase have the lower thermoelectric properties, ZT value is just about 0.4–0.6 [11–15]. Goldsmid [13] reviewed that the n-type Bi<sub>2</sub>Te<sub>3</sub> materials usually have the lower

ZT value compared to that of p-type Bi<sub>2</sub>Te<sub>3</sub> materials. Son et al. [11] reported that the nanostructured Bi<sub>2</sub>Te<sub>3</sub> synthesized by solution phase method show the ZT of 0.4 to 0.6 from the room temperature to 400 K. Li et al. [15] reported that a maximum ZT of 0.55 is obtained at 425 K for the Bi<sub>2</sub>Te<sub>3</sub>/GQDs-20 nm, which is higher than that of Bi<sub>2</sub>Te<sub>3</sub> without hybrid nanostructure. In recent years, many efforts have been made to decrease thermal conductivity especially for the lattice thermal conductivity by increase phonon scattering [16–19]. However, the typical method to reduce thermal conductivity concentrate upon nanostructuring which is adding boundary scattering and point-defect scattering that target low and high frequency phonons, such as nanoplates, nanowires, nanorods and other various nanostructure systems [20–28]. The thermal conductivity can be further decreased by introducing dense dislocation which target mid-frequency phonons [7]. Thus, here we introduced dense dislocation into grain boundaries by combining MA and SPS to scatter mid-frequency phonons. During the high temperature (728 K) which is above the melting point of Te, the excess Te was spilled out of the die. On account of Umklapp scattering, point-defect scattering, boundary scattering and dislocation scattering, an effective scattering of phonons leads to a substantially reduction of lattice thermal conductivity. The Bi<sub>2</sub>Te<sub>3</sub> + 10 wt% Te sample achieves the lowest lattice thermal conductivity of  $0.2 \text{ Wm}^{-1} \text{ K}^{-1}$  at 373 K and the highest ZT value of 0.7 at 398 K. This finding highlight that this simple process is effective to reduce thermal conductivity and obtain a high ZT value.

The commercially available high-purity powders of Bi ( $\geq 99.9\%$ ), Te ( $\geq 99.5\%$ ) were used as raw materials, which are all purchased from Alfa Aesar company without any further purification. All the powders were synthesized by mechanical alloying (MA) and the bulks were

\* Corresponding authors.

E-mail addresses: [zge@kmust.edu.cn](mailto:zge@kmust.edu.cn) (Z.-H. Ge), [hejq@sustc.edu.cn](mailto:hejq@sustc.edu.cn) (J. He).

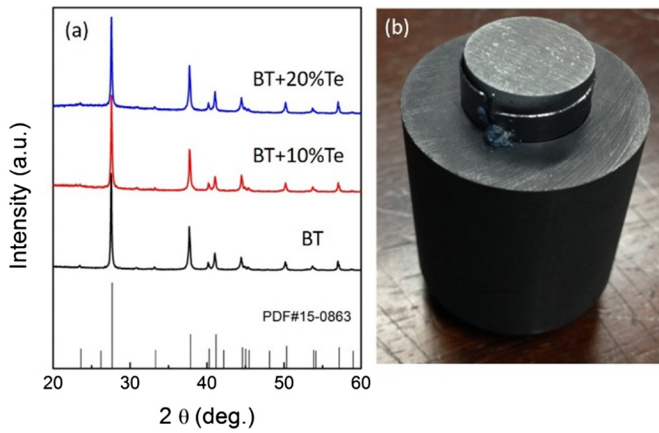


**Fig. 1.** XRD patterns of the  $\text{Bi}_2\text{Te}_3$ ,  $\text{Bi}_2\text{Te}_3 + 10 \text{ wt}\% \text{ Te}$  and  $\text{Bi}_2\text{Te}_3 + 20 \text{ wt}\% \text{ Te}$  bulk samples sintered by SPS (a) and the picture after transient liquid flow compacting process (Spark Plasma Sintering) for  $\text{Bi}_2\text{Te}_3 + 10 \text{ wt}\% \text{ Te}$  bulk sample (b).

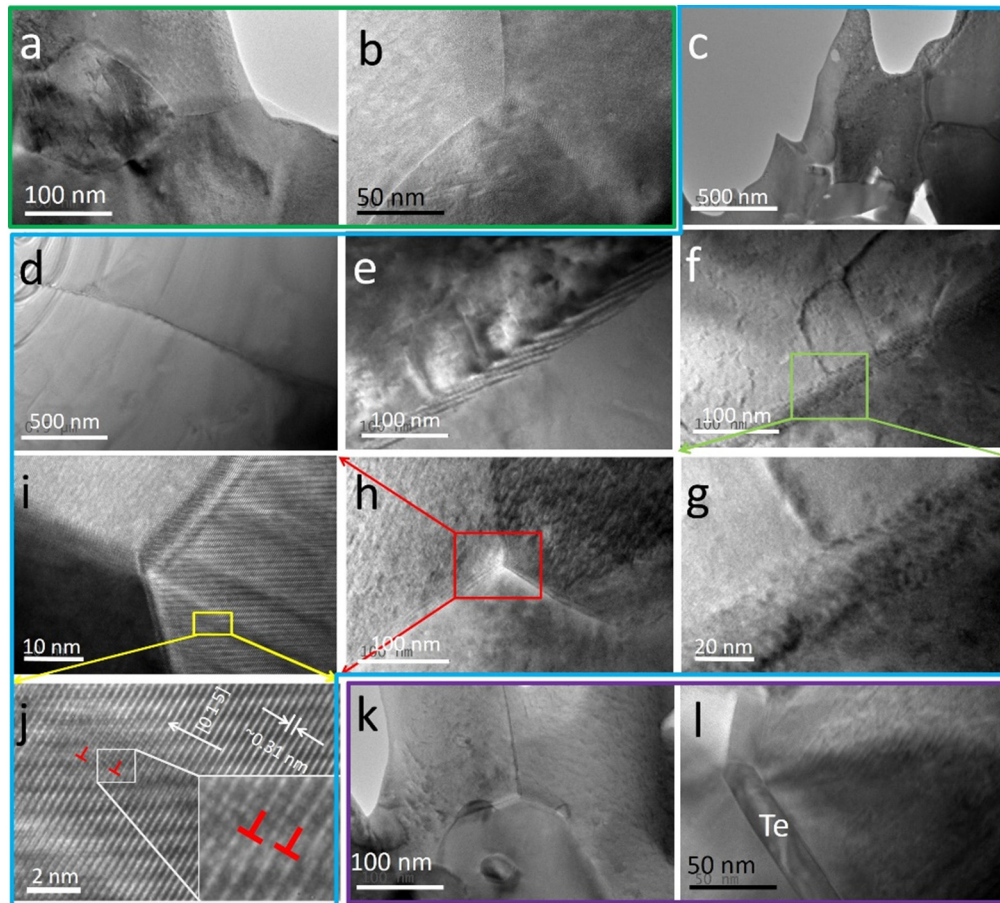
sintered by spark plasma sintering (SPS). The detail of experiment was shown in Supporting information (SI).

Fig. 1 shows the XRD patterns of all the bulk samples. According to the PDF card 15-0863, all the bulk samples are the pure  $\text{Bi}_2\text{Te}_3$  even the extra Te was added as shown in Fig. 1(a). Fig. 1(b) shows the Te was spitted out of the die and convinced our strategy. The energy dispersive spectroscopy (EDS) analysis was performed to determine the real composition of the bulk samples. As shown in Fig. S2, the  $\text{Bi}_2\text{Te}_3 + 10 \text{ wt}\% \text{ Te}$  sample has the Bi/Te ratio of 38.32 to 61.68, which is very similar to the stoichiometry

ratio of  $\text{Bi}_2\text{Te}_3$ . However, for the  $\text{Bi}_2\text{Te}_3 + 20 \text{ wt}\% \text{ Te}$  sample the element tellurium was detected, as shown in Fig. S3. The XRD could not detect the element tellurium due to the diffraction peak overlap of Te and  $\text{Bi}_2\text{Te}_3$ .

To confirm the dislocation was introduced in the grain boundary of  $\text{Bi}_2\text{Te}_3$  bulk, the transmission electron microscope (TEM) observation was performed for all the bulk samples as shown in Fig. 2. Fig. 2(a) and (b) show the low-magnification TEM image of pristine  $\text{Bi}_2\text{Te}_3$  sample, indicating the clear grain boundary. The Fig. 2(c)–(f) shows the grain boundary with dislocations of the  $\text{Bi}_2\text{Te}_3 + 10 \text{ wt}\% \text{ Te}$  sample. A clear Moiré pattern of the grain boundary can be seen in Fig. 2(g) by enlarging one view of boxed region of (f), this Moiré fringe is caused by expelled excess Te during the SPS process which can be demonstrated by contrasting with the dislocation (indicated by the red arrow) aligned along the zone axis showing only strain effects. Fig. 2(h) shows the high resolution TEM image of a triangular grain boundary of  $\text{Bi}_2\text{Te}_3 + 10 \text{ wt}\% \text{ Te}$  material. Dislocation arrays with periodic spacing of  $\sim 0.3 \text{ nm}$  along  $[0\ 1\ 5]$  crystal orientation was observed together with Moiré fringes in Fig. 2(j) and this also verifies that by expelled excess Te can introduce dislocation arrays. Fig. 2(k) and (l) shows the low-magnification TEM image of  $\text{Bi}_2\text{Te}_3 + 20 \text{ wt}\% \text{ Te}$  bulk, the Te was observed in the grain boundary. If the SPS holding time is enough, all the Te will spitted out of the die even the Te content is 20 wt%, but the holding time is set to 5 min for avoiding the grain growth to obtain the low thermal conductivity.

Thermoelectric transport properties of all the bulk sample were investigated in detail. In Fig. 3(a), the electrical conductivity for all bulk samples has a relatively high value through a wide measuring temperature range, but it has a downtrend as the temperature increase. Among the measuring temperature range, the electrical conductivity decreased dramatically, which is attributed to the fact that with the



**Fig. 2.** Low-magnification TEM image of pristine  $\text{Bi}_2\text{Te}_3$  bulk (a) and (b) (green line);  $\text{Bi}_2\text{Te}_3 + 10 \text{ wt}\% \text{ Te}$  bulk (c) to (j) (blue line): (c) to (f) low-magnification TEM image of  $\text{Bi}_2\text{Te}_3 + 10 \text{ wt}\% \text{ Te}$  bulk. (g) Enlarged view of boxed region in (f), (i) enlarged view of boxed region in (g), (j) enlarged view of boxed region in (i); and  $\text{Bi}_2\text{Te}_3 + 20 \text{ wt}\% \text{ Te}$  bulk (k) and (l) (purple line). (For interpretation of the references to colour in this figure legend, the reader is referred to the web version of this article.)

Download English Version:

<https://daneshyari.com/en/article/5443272>

Download Persian Version:

<https://daneshyari.com/article/5443272>

[Daneshyari.com](https://daneshyari.com)